Antiangiogenic AAV2 gene therapy with a truncated form of soluble VEGFR-2 reduces the growth of choroidal neovascularization in mice after intravitreal injection

Puranen, Jooseppi

2022-11

Puranen , J , Koponen , S , Nieminen , T , Kanerva , I , Kokki , E , Toivanen , P , Urtti , A , Ylä-Herttuala , S & Ruponen , M 2022 , ' Antiangiogenic AAV2 gene therapy with a truncated form of soluble VEGFR-2 reduces the growth of choroidal neovascularization in mice after intravitreal injection ' , Experimental Eye Research , vol. 224 , 109237 . https://doi.org/10.1016/j.exer.2022.109237

http://hdl.handle.net/10138/350462
https://doi.org/10.1016/j.exer.2022.109237

Experimental Eye Research 224 (2022) 109237

Contents lists available at ScienceDirect

Experimental Eye Research

journal homepage: www.elsevier.com/locate/yexer

Research article

Antiangiogenic AAV2 gene therapy with a truncated form of soluble VEGFR-2 reduces the growth of choroidal neovascularization in mice after intravitreal injection

Jooseppi Puranen [a,*,1], Sanna Koponen [b,1], Tiina Nieminen [b,c], Iiris Kanerva [b], Emmi Kokki [b], Pyry Toivanen [b], Arto Urtti [a,d], Seppo Ylä-Herttuala [b,e], Marika Ruponen [a]

[a] School of Pharmacy, Faculty of Health Sciences, University of Eastern Finland, Yliopistonranta 1, 70210, Kuopio, Finland
[b] A.I Virtanen Institute for Molecular Sciences, University of Eastern Finland, P.O Box 1627, 70211, Kuopio, Finland
[c] Kuopio Center for Gene and Cell Therapy, Kuopio, Finland
[d] Drug Research Program, Division of Pharmaceutical Biosciences, Faculty of Pharmacy, University of Helsinki, Viikinkaari 5 E, FI-00790, University of Helsinki, Finland
[e] Gene Therapy Unit, Kuopio University Hospital, 70211, Kuopio, Finland

ARTICLE INFO

Keywords:
AAV
Retinal gene therapy
Ocular neovascularization
CNV
Vascular endothelial growth factor
VEGF receptor

ABSTRACT

Pathological angiogenesis related to neovascularization in the eye is mediated through vascular endothelial growth factors (VEGFs) and their receptors. Ocular neovascular-related diseases are mainly treated with anti-VEGF agents. In this study we evaluated the efficacy and safety of novel gene therapy using adeno associated virus 2 vector expressing a truncated form of soluble VEGF receptor-2 fused to the Fc-part of human IgG1 (AAV2-sVEGFR-2-Fc) to inhibit ocular neovascularization in laser induced choroidal neovascularization (CNV) in mice. The biological activity of sVEGFR-2-Fc was determined in vitro. It was shown that sVEGFR-2-Fc secreted from ARPE-19 cells was able to bind to VEGF-A_{165} and reduce VEGF-A_{165} induced cell growth and survival. A single intravitreal injection (IVT) of AAV2-sVEGFR-2-Fc (1 μl, 4.7×10^{12} vg/ml) one-month prior laser photocoagulation did not cause any changes in the retinal morphology and significantly suppressed fluorescein leakage at 7, 14, 21 and 28 days post-lasering compared to controls. Macrophage infiltration was observed after the injection of both AAV2-sVEGFR-2-Fc and PBS. Our findings indicate that AAV2 mediated gene delivery of the sVEGFR-2-Fc efficiently reduces formation of CNV and could be developed to a therapeutic tool for the treatment of retinal diseases associated with neovascularization.

1. Introduction

Antiangiogenic treatment is one of the most effective strategies for managing pathological neovascularization in ocular diseases. Because vascular endothelial growth factors (VEGF) play a key role in pathological angiogenesis (Kinnunen et al., 2009), VEGFs and their receptors are potential targets in the treatment of ocular neovascular -related diseases. Anti-VEGF agents, such as bevacizumab, aflibercept, ranibizumab (Heier et al., 2016; Wykoff et al., 2018) and most recently brolucizumab (Dugel et al., 2020) have revolutionized the treatment of patients with neovascular ocular diseases. Although anti-VEGF therapy has become the mainstay in the treatment of neovascular ocular diseases most of the patients require frequent injections every 1–3 months interval and regular long-term follow-up, which place burden to the patients and health care (Wykoff et al., 2018). Therefore, alternative therapies with long duration of action are needed.

Ocular gene therapy is a promising approach to express anti-VEGF proteins for prolonged periods following a single injection. Several preclinical (Askou et al., 2017 and 2019, Lee et al., 2018; Ding et al., 2019) and clinical studies (Rakoczy et al., 2019; ClinicalTrials.gov NCT03585556, NCT03066258, NCT04645212, NCT03748784) demonstrate the use of anti-angiogenic gene therapy agents to inhibit pathological angiogenesis in the eye. In these studies, anti-angiogenic therapy was shown to be safe and decrease choroidal neovascularization. In clinical trials results have shown positive outcomes but also lack of efficacy (Rakoczy et al., 2019).

One of the approaches to block VEGF signalling is utilization of

* Corresponding author.
E-mail address: jooseppi.puranen@uef.fi (J. Puranen).
[1] Equal authorship.

https://doi.org/10.1016/j.exer.2022.109237
Received 3 May 2022; Received in revised form 15 July 2022; Accepted 29 August 2022
Available online 9 September 2022

Abbreviations

AAV	adeno associated virus
ARPE	human retinal pigment epithelium
BaF3	pro-B murine cell line
CMV	cytomegalovirus
CNV	choroidal neovascularization
EGFP	enhanced green fluorescent protein
IVT	intravitreal injection
nAMD	neovascular age related macular degeneration
OCT	optical coherence tomography
ONL	outer nuclear layer
sVEGFR	soluble vascular endothelial growth factor receptor
WPRE	woodchuck post-translational regulatory element

decoy receptors. VEGF-A functions are mediated by two main receptors: VEGF receptor −1 (also called *FLT1*) and VEGF receptor −2 (also called *FLK1/KDR*). Previous gene therapy experiments on treatment of neovascular age-related macular degeneration (nAMD) have focused on soluble VEGFR-1 (sVEGFR-1) constructs because it has high affinity for VEGF-A. Intravitreal delivery of an adeno-associated virus (AAV) expressing sVEGFR-1 fused to the Fc-part of IgG1 (sFLT01) (Huang et al., 2017) and subretinal delivery of an AAV vector expressing a sVEGFR-1 (sFLT) (Rakoczy et al., 2019) were safe in clinical studies. However, AAV-mediated sVEGFR-2 expression has not been tested in the treatment of ocular neovascularization.

Binding affinity of mouse VEGF-A to human VEGFR-2 has not been published. Mouse VEGF-A_{164} shares significant homology with human VEGF-A_{165} (only 19 amino acids difference) (Mujagic et al., 2013). One study reported treatment of ocular neovascularization in oxygen induced retinopathy mouse model with recombinant chimeric VEGFR-2 protein (sVEGFR-2) (Agostini et al., 2005). This protein contains the first 757 amino acids of human VEGFR-2 that were fused to human Fc. Pathological vascular changes were reduced significantly after a single intravitreal injection of sVEGFR-2. Furthermore, clinically used anti-VEGF agent aflibercept (soluble decoy receptor with human VEGFR-1 IgG domain 2 and human VEGFR-2 IgG domain 3 fused to human Fc region of IgG1) can bind mouse VEGF-A (Papadopoulos et al., 2012). Other anti-VEGF proteins bevacizumab (humanized monoclonal antibody) and ranibizumab (Fab-fragment) do not bind rodent VEGF-A efficiently (Lu and Adelman, 2009; Yu et al., 2008)

We investigated the AAV2 mediated retinal gene transfer after intravitreal injection to establish long-term production of truncated form of sVEGFR-2 for the treatment of choroidal neovascularization. More precisely, we used sVEGFR-2-Fc which is a recombinant fusion protein composed of the 1–3 Ig domains of VEGFR-2 fused to the Fc region of human immunoglobulin gamma 1 (IgG1) (Fig. 1) to ensure dimerization of the soluble receptors. The Fc fusion proteins are homodimers and they can improve the solubility and stability of the receptors (Czajkowsky et al., 2012). The dimerization of VEGF receptors is required for their high-affinity binding to VEGF-A (Sallinen et al., 2011). The efficacy of AAV2-sVEGFR-2-Fc against CNV formation and ocular safety of the transgene expression was evaluated in a mouse model of laser-induced choroidal neovascularization which mimics many of the abnormalities seen in the nAMD. This study is the first attempt to test AAV2-sVEGFR-2 gene therapy as a therapeutic tool for CNV -related diseases.

2. Materials and methods

2.1. Production of AAV-vectors

AAV plasmid containing codon optimized sequences encoding VEGFR2 extracellular Ig like domains 1, 2 and 3 and human IgG1 Fc-fragment (pAAV-sVEGFR-2-Fc) was synthetized by Life Technologies. AAV Serotype 2 expressing Enhanced green fluorescent protein (AAV2-EGFP) with CMV promoter and Woodchuck Posttranscriptional Regulatory Element (WPRE) and AAV2-sVEGFR-2-Fc with CMV promoter vectors were produced as described previously by Zolotukhin et al. (1999). HEK293T cells were co-transferred with a vector plasmid and a helper plasmid pDG. Vectors were purifiedby iodixanol gradient centrifugation and 40% iodixanol step with Amicon. Functional titration of AAV2-EGFP was determined using a slot blot and flow cytometry as described previously by Paterna et al. (2000) Vector titers for AAV2-EGFP (2.8×10^{12} vg/ml) and for AAV2-sVEGFR-2-Fc (4.7×10^{12} vg/ml) were determined with functional qPCR as described earlier (Suoranta et al., 2021) using inverted terminal repeat (ITR) specific primers.

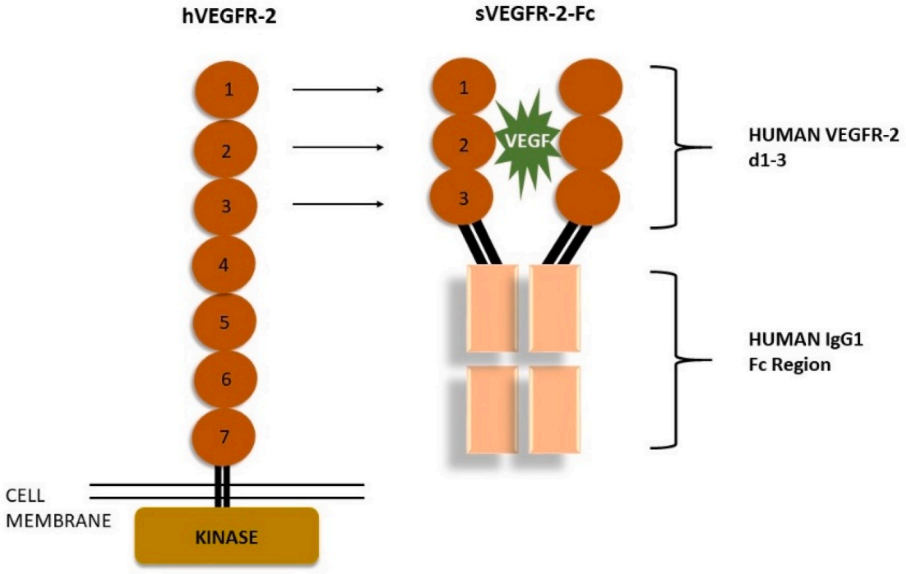

Fig. 1. sVEGFR-2-Fc was constructed by fusing the first, second and third (D1-D3) Ig-like domains of VEGFR-2 to the Fc portion of human IgG1. Abbreviations: VEGF, vascular endothelial growth factor; sVEGFR, soluble VEGF receptor; Ig, immunoglobulin.

2.2. Cell transduction

Human retinal pigment epithelium (ARPE-19) cells were cultured on 6-well plates at 75 000 cells per well in Dulbecco's modified Eagle's minimum essential medium (DMEM) (Gibco) supplemented with 10% fetal bovine serum (FBS) (Gibco) and 1% penicillin/streptomycin (Gibco) and incubated at 37 °C in a humidified atmosphere with 5% CO2. Transduction of the cells was performed with AAV2-sVEGFR2-Fc vector at multiplicity of infection (MOI) 20 000, 100 000 and 1000 000. Medium was changed the following day. Three days post-transduction, transduction medium was collected and stored at −70 °C prior to be tested by Western blot and ELISA.

2.3. Western blotting and SDS-PAGE

The secreted sVEGFR-2-Fc protein from the medium collected from AAV2-sVEGFR2-Fc transduced ARPE-19 cells was detected by Western blot. Samples were denaturated for 5 min at 95 °C under reducing conditions and proteins were separated by sodium dodecyl sulfate–polyacrylamide gel electrophoresis (SDS-PAGE) (4–20% Mini-Protean TGX Stain Free Gel, Bio-Rad). Proteins were transferred to nitrocellulose membrane (Nitrocellulose Membrane 0.2 μm, Trans-Blot Turbo, Bio-Rad) and blocked in 5% milk in 1 × TBS and 0.1% Tween. Blot was incubated first with Anti-Human IgG (Fc specific) antibody (I2136, Sigma-Aldrich) and then with Donkey Immunoglobulin G HRP conjugated secondary antibody (DkxGt-003-DHRPX, ImmunoReagents, Inc). Bands were visualized using Pierce ECL Plus Western Blotting Substrate (Thermo Scientific) and detected with ChemiDoc MP (Bio-Rad) imager.

2.4. Binding assays

Enzyme-linked immunosorbent assay (ELISA) was used to determine the capability of sVEGFR-2-Fc to bind recombinant human VEGF-A_{165}. Wells of 96-well plates were coated with VEGF-A_{165} (5 μg/ml) (293-VE, R&D Systems) in bicarbonate buffer (0,1M NaHCO3) overnight. Blocking was done with 0.5% BSA in Phosphate Buffered Saline with Tween™ 20 (PBST) for 1.5 h. Dilution series of medium containing sVEGFR-2-Fc collected from the transduced ARPE-19 cells was added to the plates and incubated for 1 h following incubation with anti-human IgG-HRP antibody for 1 h (Anti Human IgG Peroxidase conjugate, A8792, Sigma). 3,3′, 5,5″-tetramethylbenzidine (TMB) substrate solution (N301, Thermo-Fischer) was added to the plates and incubated for 20 min, and reaction was stopped by adding stop solution (N600, Thermo-Fischer). Absorbance was measured at 450 nm wavelength.

2.5. BaF3-VEGFR-2 viability assay

BaF3 (BaF3-VEGFR-2) cells expressing VEGFR-2/EpoR described by Achen et al. (1998) (received as a generous gift from Dr. Alitalo) were cultured in DMEM (Gibco) supplemented with 10% FBS (Gibco), 1% penicillin/streptomycin (Gibco), 500 μg/ml Geniticin (G418, InvivoGen) and recombinant mouse interleukin-3 (rmIl-3) (407 631, EDM-Millipore). For the viability assay, 18000 cells per well were cultured on 96-well plates in the medium containing 25 ng/ml VEGF-A_{165} (293-VE, R&D Systems) without rmIl-3 and with dilution series of medium containing sVEGFR-2-Fc collected from the transduced (100 000) ARPE-19 cells. Recombinant sVEGFR-2 described earlier (Toivanen et al., 2009) was used as a positive control. After 48 h of incubation at 37 °C in a humidified atmosphere with 5% CO_2, cell viability was quantified by adding CellTiter 96® AQueous One Solution Cell Proliferation Assay (MTS) (G3582, Promega) to the wells and plates were incubated 2 h. After the incubation, absorbances were measured using 490 nm wavelength.

2.6. Animals

Eight to 10-weeks old male C57BL/6J mice (Lab Animal Center, Kuopio, Finland) were used in this study. All animals were treated in standard conditions under a 12-h light/dark cycle with food and water available *ad libitum*. Animal experiments were conducted in accordance with the Association for Research in Vision and Ophthalmology statement for the Use of Animals in Ophthalmic and Vision Research and was approved by the Finnish National Animal Experiment Board (ESAVI-2020-027 769). All animal experiments were conducted under anesthesia by intraperitoneal injection of 60 mg/kg ketamine (Ketaminol®, Intervet International B.V.) and 0.4 mg/kg medetomidine (Domitor®, Orion Oy, Finland). The pupils were dilated with topical application of 0.5% tropicamid (Santen Pharmaceuticals Co, Ltd., Tampere, Finland). The effect of anesthetics was reversed with 1 mg/kg atipamezole (Antisedan®, Orion Oy, Finland) given subcutaneously. In vivo study design is presented in Fig. 2.

2.7. Laser-induced choroidal neovascularization model

Mice were anaesthetized and pupils were dilated as described above. The animals were positioned in front of a slit-lamp and the beam from a diode laser (Vitra 2; Quantal Medical, Rockwall, TX, USA) was focused onto the retina. Both eyes of each mouse were subjected to laser photocoagulation and four laser burns were placed around optic nerve head in each eye (spot size 50 μm, duration 0.1 s, power 50 mW). The lesions were located at the 3, 6, 9 and 12 o'clock centered on the optic nerve head and located approximately three-disc diameters from the optic disc. Acute vapor bubbles formed at the laser spots indicated the rupture of Bruch's membrane. Mice with hemorrhage were excluded from the further studies.

Experimental choroidal neovascularization (CNV) model was validated with intravitreal injection of aflibercept (Eylea®, 40 mg/ml, Regeneron Pharmaceuticals, Tarrytown, NY, USA) as illustrated in Fig. 2A. Immediately after photocoagulation 40 μg of aflibercept (1 μl, n = 10) as positive control or PBS (Dulbecco's Phosphate-Buffered Saline, ThermoFisher Scientific) (pH 7.4, 10 mM, n = 8) as negative control were injected into vitreous cavity (n = 10). Proper placement of the compound was confirmed with optical coherence tomography (OCT). Efficacy of aflibercept treatment on CNV development was evaluated with fluorescein angiography on days 7, 14, 21 and 28. Efficacy of PBS was evaluated with fluorescein angiography on day 7. Fluorescein leakage areas were compared to equal number of lasered non-treated controls.

2.8. Intravitreal AAV administration

AAV2-sVEGFR-2-Fc. Total of 20 mice were randomly divided into two groups (n = 10 per group). Group 1 received intravitreal (IVT) injection of AAV2- sVEGFR-2-Fc with CMV promoter (1 μl, 4.7×10^{12} vg/ml). Group 2 did not receive intravitreal injections and acted as control. Briefly, mice in group 1 were anaesthetized and pupils were dilated with tropicamide eye drops. Topical analgesia was given prior injections with oxybuprocaine (Oftan Obucain, 4 mg/ml, Santen Oy, Finland) eyedrops. AAV vectors were administered into vitreous cavity using 32G needle fitted with Hamilton syringe (Hamilton Co., Reno, NV, USA). Both eyes were treated. The needle was directed toward the center of the vitreous and volume of 1 μl was slowly injected. A topical eye drop (Viscotears®, Alcon, Finland) was applied to the eyes of mice immediately after IVT injection avoiding any material leakage from the vitreous. Quality of IVT injections was confirmed with optical coherence tomography (OCT) and fundus images (Micron IV; Phoenix Research Labs, Pleasanton, CA, USA). Laser photocoagulation was performed four weeks after IVT injection. Efficacy was monitored with fluorescein angiography (FA) and CNV size analysis. The experimental setup is presented in Fig. 2B. For sVEGFR-2-Fc protein expression analyses the animals received

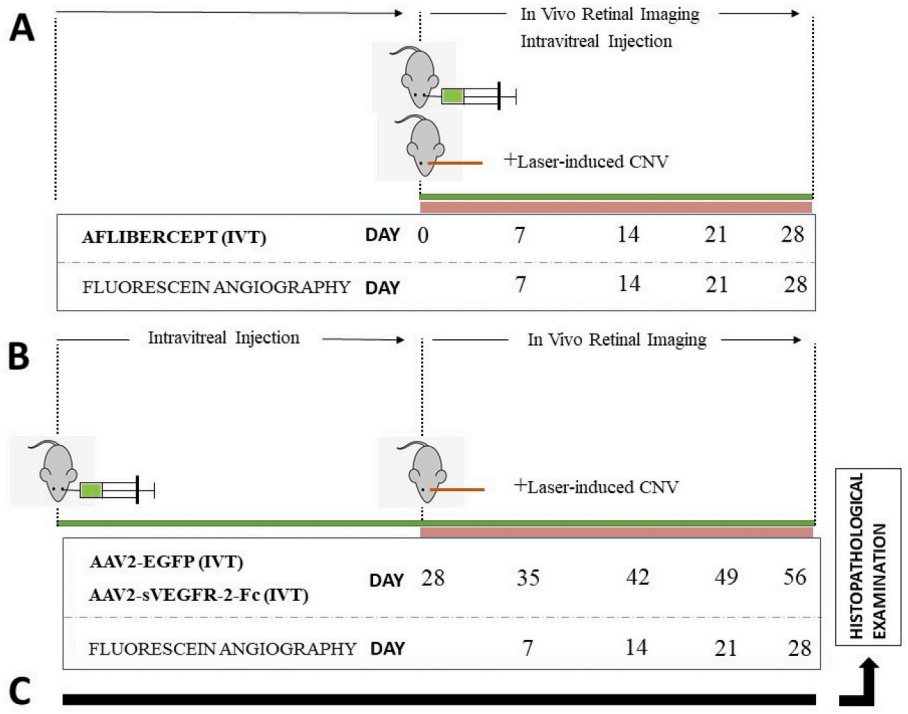

Fig. 2. In vivo part of the study was divided into three experimental arms (A, B and C). **A.** The CNV mouse model was validated with single intravitreal injection of aflibercept and phosphate buffer. Photocoagulation was done immediately after intravitreal treatment. The inhibitory effects of aflibercept on CNV development was confirmed with fluorescein angiography measurements at 7, 14, 21 and 28 days after intravitreal administration. **B.** In the second study the efficacy of AAV2-sVEGFR-2-Fc to CNV formation was examined in the CNV mouse model. Laser photocoagulation was induced 28 days after the intravitreal injection of AAV2-sVEGFR-2-Fc vectors to allow sufficient time for transgene expression. Fluorescein angiography was done at days 7, 14, 21 and 28 post-lasering. Fluorescein angiography and OCT data was used for efficacy analysis. Mice were sacrificed and eyes were collected for histopathological examinations 56 days after AAV2-sVEGFR-2-Fc administration. Parallel to the study, intraocular expression of EGFP following by intravitreal injection of AAV2-EGFP was examined. Transgene expression profile was visualized by green-filter fundus photography at days 14, 21, 49 and 63 post intravitreal injection and with anti-GFP immunostaining. **C.** Ocular tolerability and immune response examinations were made with retinal layer measurements (ONL thickness) and immunohistochemical analysis. Four different experimental groups were used in this study. Mice in group 1) and 2) received IVT injection of AAV2-sVEGFR-2-Fc (1 μl) or PBS-buffer (1 μl), respectively. Mice in Group 3) got no IVT injections and were treated with laser (laser group; four laser spots per eye) and mice in group 4) were naïve. Mice were sacrificed 56 days after the treatments. IVT = intravitreal administration. (For interpretation of the references to colour in this figure legend, the reader is referred to the Web version of this article.)

intravitreally AAV2-sVEGFR-2-Fc (3.2×10^{12} vg/ml; 2 μl) into both eyes. Procedure was done similar as for group 1. These animals were not subjected to OCT, FA or laser photocoagulation procedures.

AAV2-EGFP. AAV2-EGFP (2.8×10^{12} vg/ml) was injected into vitreous as described above (n = 5 mice). Enhanced green fluorescent proteins were visualized using fundus camera with green filter at days 14, 21, 49 and 63 post-treatments.

2.9. Fluorescein fundus angiography

Fluorescein angiography was performed to anaesthetized mice using Micron IV imaging system (Micron IV; Phoenix Research Labs, Pleasanton, CA, USA) at 7, 14, 21 and 28 days after laser photocoagulation. Photographs were captured in contact with fundus camera lens at 10-s intervals after subcutaneous injection with 0.1 ml of 1% fluorescein sodium (Alcon Laboratories Inc., Fort Worth, TX, USA). Late phase images (5 min) were used for comparative analyses. The area of fluorescein leakage was calculated as number of pixels by ImageJ software (National Institute of Health, Bethesda, MD, USA). Total of 80 fluorescein leakage areas per group for each timepoint were analysed (n = 10 mice per group, both eyes were treated and each eye had 4 laser spots).

2.10. Analysis of CNV area

ImageJ software was used to delineate and measure the CNV area from OCT pictures (ImageJ, National Institute of Health, Bethesda, MD, USA). CNV size was defined as the subretinal hyperreflective material above retinal pigment epithelium layer. Cross-sectional areas passing through the lesion were manually contoured, and measurements were performed in all laser photocoagulation sites. Maximum lesion size of the CNV was included in the data set.

2.11. Ocular tolerability to AAV2-sVEGFR-2-Fc gene therapy in choroidal neovascularization mouse model

The mice were monitored for AAV2-sVEGFR-2-Fc treatment related ocular toxicities (Fig. 2C). Toxicity examinations included retinal layer measurements (Outer nuclear layer thickness, ONL) and immunohistochemical analyses. In this study, the mice were divided into four groups (n = 4 mice in each group). Mice in groups 1 and 2 received IVT injections of AAV2-sVEGFR-2-Fc (1 μl, 4.7×10^{12}) or PBS-buffer (1 μl, 1xPBS pH 7.4), respectively. Mice in Group 3 did not receive any IVT injections but were treated with laser (laser group; four laser spots per eye) and mice in group 4 were naïve.

Image based quantitative analysis of ONL thickness. The mice were anaesthetized and pupils were dilated with 0.5% tropicamide eye drops. Mice were placed in a holder in front of OCT imaging device and the eyes were moisturized with Viscotears™ (Alcon, Finland). High resolution OCT (Micron IV; Phoenix Research Labs, Pleasanton, CA, USA) was performed with a line scan protocol (line scans of 0°, composed of 20 images) before and 8 weeks after the IVT injection. Segmentation of the retinal layers was performed automatically with in-built software (InSight, version 2.0.5940). OCT imaging was performed on two regions of each eye using the optic disc as a reference point, one on the superior side of the optic disc and one on the inferior side. Only b-scans with straight entry position of the OCT beam to retina were chosen for analysis. Automatically drawn segmentation lines were checked and manually corrected when needed. The area between outer plexiform layer and the external limiting membrane displayed the mean ONL thickness.

Histopathological examination. The mice were sacrificed and eyes were collected for histopathological examinations 56 days after the AAV2-sVEGFR-2-Fc. The eyes were preserved in 4% paraformaldehyde in 0.1M phosphate buffer (pH 7.4) for overnight at 4 °C. The eyes were

embedded into paraffin and sagittal sections (5 μm thickness) were cut with a microtome (Leica Microsystems, Nussloch GmbH, Germany). The sagittal sections were stained with Anti-GFP Antibody ((FL): sc-8334, Santa Cruz Biotechnology, Inc.) to confirm the EGFP expression in the retina. Antibody F4/80 (Rat anti Mouse F4/80 antibody, clone A3-1, MCA497G, Bio-Rad) was used to detect macrophages in the eye. Presence or absence of immunopositivity was evaluated blindly by examining 9 sections sectioned at different levels of each eye using a brightfield microscope (Nikon Eclipse Ni-e, Nikon Instruments Europe B. V, manufactured in Japan). F4/80 positive cells in the retina and vitreous were counted manually.

2.12. sVEGFR-2-Fc protein expression in the mouse eye after intravitreal injection of AAV2-sVEGFR-2-Fc

Expression of sVEGFR-2-Fc protein levels were studied by ELISA. The proteins were extracted from whole eye samples collected at timepoints 2 weeks (n = 3) and 6 weeks (n = 3) after the intravitreal injection of AAV2-sVEGFR-2-Fc. Naïve animals were used as controls (n = 4). The eyes (~50 mg, 2 eyes pooled together) were lysed with buffer (cOmplete™ EDTA free protease inhibitor cocktail tablets, Roche; T-PER Tissue Protein Extraction, Thermo Scientific). Bicinchoninic acid (BCA)-protein assay (Pierce™ BCA Protein Assay Kit, Thermo Scientific™) was used to determine the total protein content of the samples. ELISA was used to quantify the sVEGFR-2 protein in the samples according to the manufacturer's protocol (Human VEGFR2/KDR Quantikine ELISA Kit, cat.no. DVR200, R&D Systems). Absorbances were measured at 450 nm and 540 nm wavelengths and normalized to the total protein content.

2.13. Statistical analysis

Statistical data were analysed with SPSS (v. 27, SPSS Inc., Chicago, USA). Two group comparisons were performed using a non-parametric test (Mann-Whitney *U* test). Results were expressed as the mean ± SEM. Differences were considered significant when $p < 0.05$.

3. Results

3.1. AAV2-sVEGFR-2-Fc efficiently transduces ARPE-19 cells

To show that AAV2-sVEGFR-2-Fc is able to transduce ARPE-19 cells and sVEGFR-2-Fc protein is secreted to the medium, immunoblotting was performed from medium collected from AAV2-sVEGFR-2-Fc transduced ARPE-19 cells (n = 2). sVEGFR-2-Fc was highly expressed with the used MOI's and no sVEGFR-2-Fc was detected in non-transduced cells (Fig. 3A).

3.2. sVEGFR-2-Fc binds to VEGFA$_{165}$ and reduces VEGF-A$_{165}$ induced cell growth and survival

Binding of sVEGFR-2-Fc to VEGF-A$_{165}$ was determined using ELISA. Dilution series of sVEGFR-2-Fc containing medium from transduced ARPE-19 cells showed specific binding to VEGF-A$_{165}$ coated plates, but no binding to VEGF-A$_{165}$ was detected with medium collected from non-transduced cells or plates without coating (Fig. 3B). Binding was reduced with higher dilutions of the medium. The effect of sVEGFR-2-Fc on VEGF-A$_{165}$ induced BaF3-VEGFR2 cell proliferation and survival was also evaluated. VEGF-A$_{165}$ induced cell growth and viability was reduced by increasing amounts of sVEGFR-2-Fc containing medium from the transduced ARPE-19 cells, similar to higher concentrations of the positive control (recombinant sVEGFR-2-Fc), but no change was observed with medium collected from the non-transduced cells (Fig. 3C.)

3.3. Single intravitreal injection of aflibercept suppresses fluorescein leakage for 7 days in CNV mouse model

Validation of the CNV mouse model was done by a single IVT administration of aflibercept (40 μg). Aflibercept significantly suppressed fluorescein leakage 7 days post photocoagulation (Fig. 4). There was no statistically significant difference between the control and aflibercept-treated group after 7-day timepoints. Intravitreally administered PBS (negative control) did not suppress fluorescein leakage 7 days post treatment (Fig. S1).

3.4. AAV2 mediated soluble VEGFR-2-Fc gene transfer suppresses the choroidal neovascularization after intravitreal administration

The AAV2-EGFP (2.8×10^{12} vg/ml) vector was injected intravitreally and the changes in GFP expression in the retinas of live mice were followed by green filter fundus camera (Fig. 5A). GFP expression was confirmed 1 week after the injection and intensity gradually increased from 1 to 9 weeks (63 days). Expression pattern was more prominent around the optic disk and the center of the retina and distributed to the injection site. Enhanced vector transduction was shown to locate in various cells of the inner nuclear layer after intravitreal administration (Fig. S2).

Mice treated with a single intravitreal injection of AAV2-sVEGFR-2-Fc (4.7×10^{12} vg/ml) showed a significantly suppressed fluorescein leakage at 7, 14, 21 and 28 days post-lasering (Fig. 5B). The fluorescein

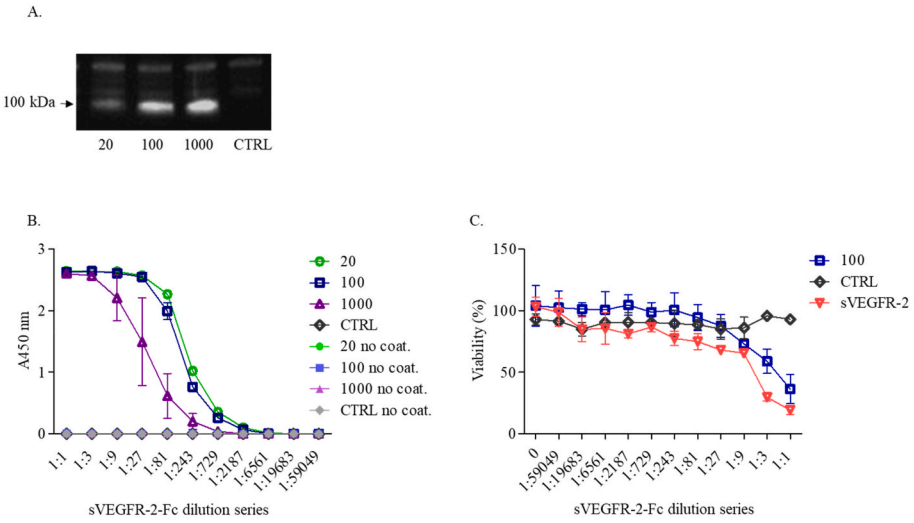

Fig. 3. A. sVEGFR-2-Fc protein expression. sVEGFR-2-Fc expression was detected in AAV2-sVEGFR-2-Fc transduced ARPE-19 cell medium with MOIs 20 000 (20), 100 000 (100) and 1000 000 (1000), and not in the medium collected from non-transduced cells (CTRL). **B.** Binding of sVEGFR-2-Fc to VEGF-A$_{165}$. Secreted sVEGFR-2-Fc bound to VEGF-A$_{165}$ coated wells at all used MOIs: 20 000 (20), 100 000 (100) and 1000 000 (1000). No binding was seen when the medium of non-transduced cells (n = 2 wells/sample) or non-VEGF-A$_{165}$ coated wells (no coat.) was used. **C.** VEGF-A$_{165}$ induced BaF3-VEGFR-2 cell growth and viability was reduced in the presence of sVEGFR-2-Fc containing medium (100 000 (100) MOI's) and recombinant sVEGFR-2 (dilution start concentration 20 μg/ml) (positive control), and not in the presence of medium collected from non-transduced cells (CTRL) (n = 2 wells/sample).

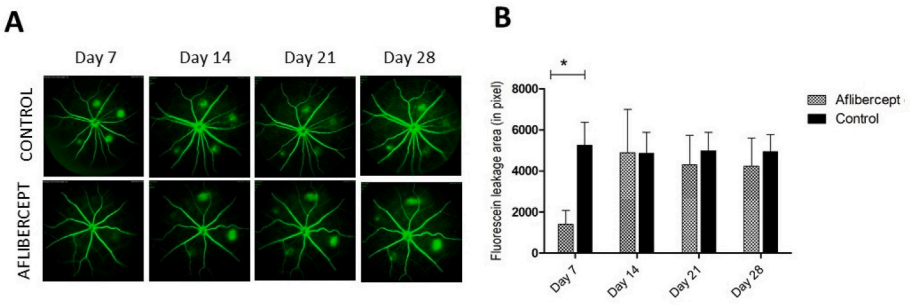

Fig. 4. Fluorescein angiography of single intravitreal administration of aflibercept (dose 40 μg). **A.** Representative fluorescein angiography photos from aflibercept (photocoagulation and intravitreal treatment) and control mice (photocoagulation only) at 7, 14, 21 and 28-day post lasering. **B.** A diagram showing the fluorescein leakage areas from aflibercept and control group at 7-, 14-, 21- and 28-day timepoints. The data is presented as mean ± SEM (n = 80 fluorescein leakage areas per group for each timepoint). * denotes statistically significant difference compared to the controls ($p < 0.05$).

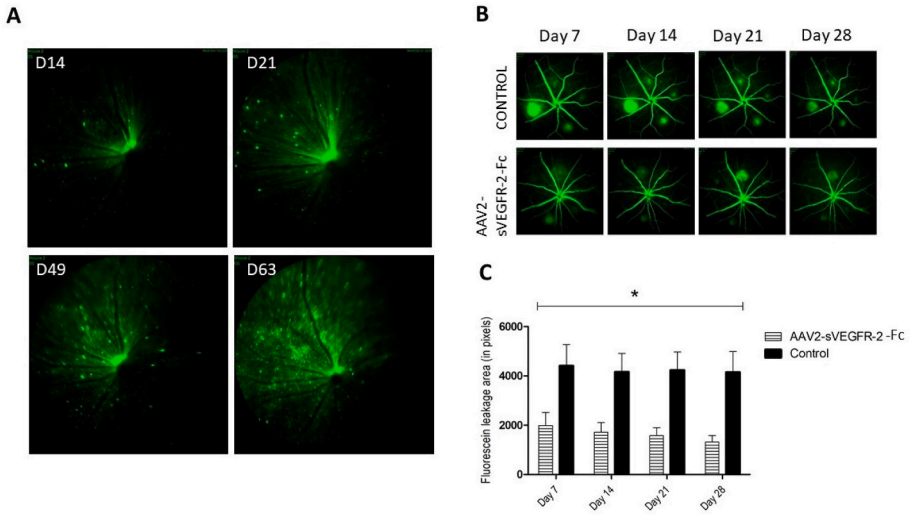

Fig. 5. A. Intraocular transgene expression at 14, 21, 49 and 63 days after intravitreal injection of AAV2-EGFP. **B**. Representative fluorescein angiography photos from AAV2-sVEGFR-2-Fc (photocoagulation and intravitreal treatment) and control (photocoagulation only) mice at 7, 14, 21 and 28-day post lasering. **C.** A diagram showing the fluorescein leakage areas from AAV2-sVEGFR-2-Fc and control group at 7-, 14-, 21- and 28-day timepoints. The data is presented as mean ± SEM (n = 80 fluorescein leakage areas per group for each timepoint). * denotes statistically significant difference compared to the controls ($p < 0.05$).

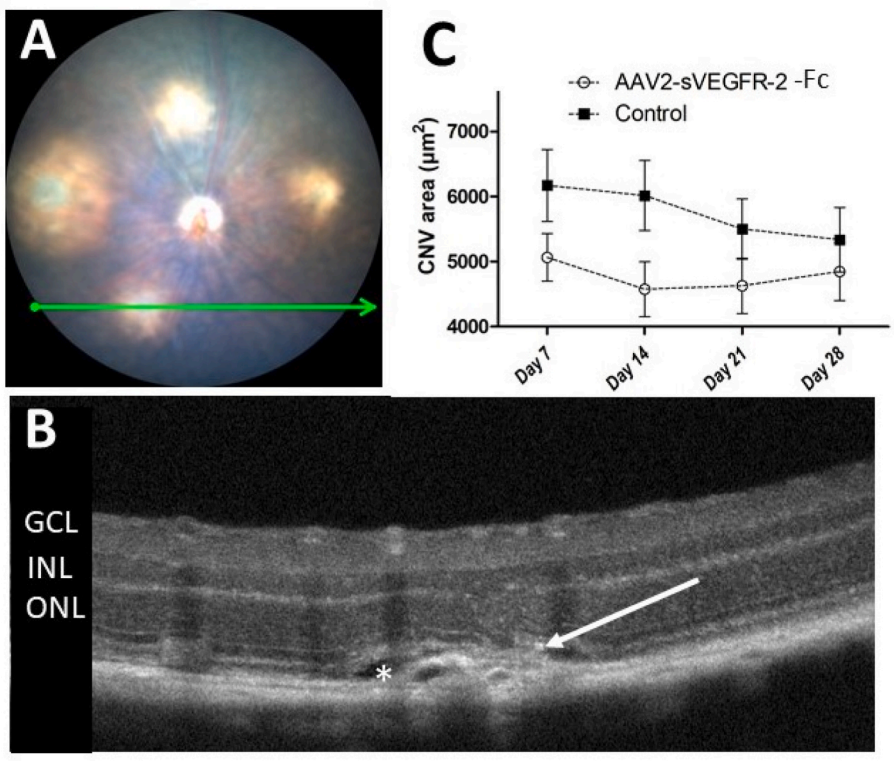

Fig. 6. A. Color fundus photography from the mouse CNV model. Green arrow indicates the plane of OCT image. **B.** OCT image from laser-induced CNV lesions. White arrow illustrates the subretinal hyper-reflective material used for data analysis (CNV area). Asterix indicates the presence of subretinal fluid. **C.** A diagram represents CNV areas calculated from AAV2-sVEGFR-2-Fc and the control groups. All data presented as mean ± SEM (n = 80 fluorescein leakage areas per group for each timepoint). GCL = ganglion cell layer, INL = inner nuclear layer, ONL = outer nuclear layer. (For interpretation of the references to colour in this figure legend, the reader is referred to the Web version of this article.)

leakage area was more than 50% smaller in the AAV2-sVEGFR-2-Fc treated group compared to the control group at all timepoints (Fig. 5C).

To confirm whether the decrease in the leakage in fluorescein angiography is a consequence of the suppression of CNV, we analysed CNV areas also from the OCT pictures (Fig. 6). The results revealed that CNV areas were smaller in eyes treated with AAV2-sVEGFR-2-Fc compared with those in the controls at days 7, 14, 21 and 28.

3.5. Outer nuclear layers are well preserved in the retina eight weeks after intravitreal administration of AAV2-sVEGFR-2-Fc

The relative thickness of the ONL was measured from OCT pictures to assess the relationship between AAV2-sVEGFR-2-Fc treatment and photoreceptor death. Fig. 7 shows the typical examples from the automatic segmentation of the ONL layer. The average outer nuclear layer thickness was 72 ± 2 μm in all groups. The average ONL thickness in AAV2-sVEGFR-2-Fc treated mice was not significantly thinner than in the controls ($p > 0.05$), indicating that the AAV2-sVEGFR-2-Fc treatment did not cause any changes in the retinal morphology that could be detected with OCT.

3.6. Elevated number of F4/80 (+) cells in the retina eight weeks after intravitreal administration of AAV2-sVEGFR-2-Fc

The recruitment of macrophages after intravitreal injections and photocoagulation was assessed by counting F4/80 positive cells per retinal section manually (Fig. 8). The F4/80 positive cells were visible in all groups. Single intravitreal injection of PBS showed a moderate (grading ++) F4/80- positive cell count compared to untreated naïve animals (grading +). Eyes treated with AAV2-sVEGFR-2-Fc showed a higher positive cell count (grading +++) compared to any other groups.

3.7. sVEGFR-2-Fc protein is expressed in the mouse eye after intravitreal administration of AAV2-sVEGFR-2-Fc

sVEGFR-2 protein was expressed two and six weeks after the intravitreal injection of AAV2-sVEGFR-2-Fc (3.2×10^{12} vg/ml, 2 μl/eye). No sVEGFR-2-Fc protein expression was detected in naïve animal (Fig. 9). The level of sVEGFR-2 protein was approximately two times higher at six weeks than at two weeks after injection.

4. Discussion

Our findings demonstrate that AAV2-mediated delivery of sVEGFR-2-Fc reduces formation of laser induced CNV in mice. In addition, one study report containing genome editing of VEGFR2 by using CRISPR-CAS has shown suppression of neovascularization in laser induced CNV mice (Huang et al., 2017). These results shed light on the development of VEGFR-2 based therapy for the wet form of AMD and possibly other ocular neovascular diseases.

In this study AAV2 was selected as carrier of sVEGFR-2-Fc, because AAV2 has shown to transduce retina efficiently in the previous studies (Kalesnykas et al., 2017; Lee et al., 2018) and sub-retinal voretigene neparvovec-rzyl (Luxturna) has already been approved by the FDA in 2017 for the treatment of rare inherited retinal disease. We investigated the intravitreal route of gene delivery due to its potential ease of clinical use as compared to the subretinal injections.

Human VEGFR-2 is composed of seven extracellular immunoglobulin-like domains (D1-D7) of which subunits D2 and D3 serve as the binding sites for activating ligands. VEGFR-2 binds the A, C and D isomers of human VEGF, it has relatively selective expression in the endothelial cells and it is upregulated during pathological angiogenesis ((Shibuya et al., 2011). VEGFR-2 exists both as transmembrane form and sVEGFR-2. As VEGFR-2 traps and inhibits VEGF-C and VEGF-D, this receptor functions also as a key regulator in the development and growth of lymphatic vessels. In functional in vivo studies, sVEGFR-2 was demonstrated to play a pivotal role in inhibiting angiogenesis in various tumours (Collet et al., 2013; Kou et al., 2004; Wu et al., 2006) and dysregulation has been associated with different pathological processes in the eye (Noma et al., 2011). These results suggest that sVEGFR-2 therapy may have potential in the treatment of ocular neovascular diseases. The function of sVEGFR2-Fc is mainly inhibitory, complexing VEGF and thus acting as a regulator of VEGF-A, –C and -D bioavailability. Furthermore, it can form heterodimers with wild type VEGFR-2 and block the activity by competitive suppression (Millauer et al., 1996).

The efficacy of the AAV2-sVEGFR-2-Fc was confirmed in a mouse model of ocular neovascularization. Retinal laser treatment was done 4 weeks after the intravitreal injection of AAV2-sVEGFR-2-Fc to allow a sufficient time for the transgene expression. Following laser treatment, the efficacy of sVEGFR-2-Fc therapy against CNV was demonstrated by (i) fluorescein angiography and (ii) quantitative OCT analysis. All the animals treated with the AAV2-sVEGFR-2-Fc had reduced fluorescein leakage compared to the control eyes. Single intravitreal injection suppressed fluorescein leakage for 28 days. Additionally, the size of CNV tended to be reduced compared to the CNV size in the control eyes, although this was not statistically significant. This may reflect the fact that the diameter of the CNV on the cross-sections is difficult to measure due to the diffuse boundaries of the CNV.

Aflibercept treatment supressed leakage of vessels only for 7 days; presumably due to its rapid elimination from the eye. Aflibercept is similar in size to sVEGFR-2-Fc (molecular weight ~110 kDa) and based on molecular sizes their estimated intravitreal half-lives are in the range of 20–40 h in mice (Schmitt et al., 2019) and 7 days in humans (Stewart, 2011). Therefore, a single intravitreal administration of aflibercept can inhibit ocular angiogenesis for one week in mice (Fig. 4) and one month in humans (Carrasco et al., 2020). The disparity in the half-lives is due to the size differences of the eyes (Schmitt et al., 2019). The size of mouse vitreous is only 5 μl (compared to 4 ml in human eye). Prolonged action after gene transfer is attributed to the continuous secretion of the transgene product from the transfected retinal cells. In previous study it was shown that AAV2 mediated gene delivery of GFP tranduces cells in

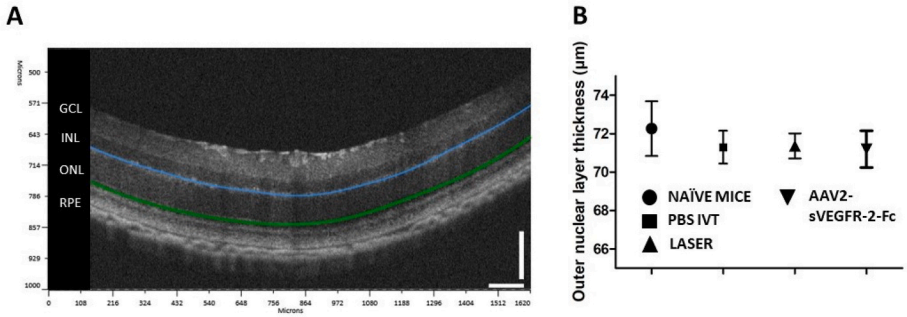

Fig. 7. A. Segmentation of retinal layers with Insight® software. Blue line denotes outer plexiform layer, green line shows external limiting membrane. **B.** Comparison of the thickness of the outer nuclear layer between naïve, PBS-IVT (intravitreally injected PBS), laser (photocoagulation only) and AAV2-sVEGFR-2-Fc treated groups. Data is presented as mean ± SD (n = 8 eyes per group). (For interpretation of the references to colour in this figure legend, the reader is referred to the Web version of this article.)

A

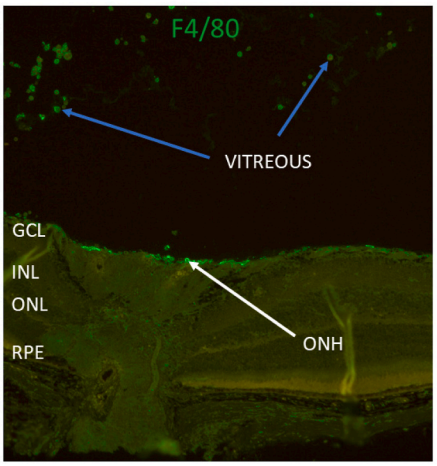

B

The recruitment of F4/80 positive cells in the eye

GROUP	F4/80
NAIVE	+
LASER	+
PBS IVT	++
AAV2-sVEGFR-2-Fc	+++

Fig. 8. A. Representative pictures from retinal sections from AAV2-sVEGFR-2-Fc treated mice eight weeks after the intravitreal injection. Immunofluorescent labelling with F4/80 (green) is shown. Blue arrows indicate the F4/80 positivity in vitreous and white arrow indicates the F4/80 positivity in optic nerve head (ONH). **B.** The number of F4/80-positive cells in the eye per section: 1–9 (+), 10–35 (++), >36 (+++). Laser = photocoagulation treated mice. GCL = ganglion cell layer, INL = inner nuclear layer, ONL = outer nuclear layer, RPE = retinal pigment epithelium. (For interpretation of the references to colour in this figure legend, the reader is referred to the Web version of this article.)

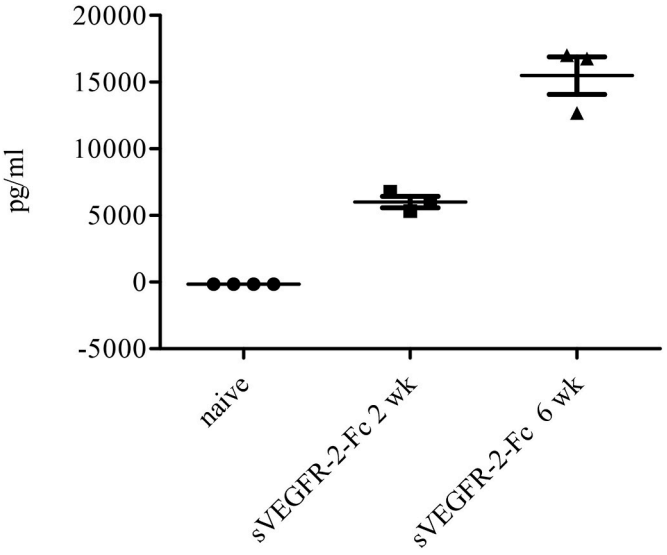

Fig. 9. The sVEGFR-2-Fc expression in the mouse eye samples two and six weeks after intravitreal injection of AAV2-sVEGFR-2-Fc. Higher levels of sVEGFR-2-Fc expression were detected at 2-week (n = 3) and 6-week (n = 3) timepoints compared to the naïve animals (n = 4).

retinal pigment epithelium, ganglion cell layer, inner nuclear layer, inner and outer plexiform layer (Kalesnykas et al., 2017).

The AAV vectors do not cause human or animal diseases, they exert low toxicity and provide a long-term gene expression (MacLachlan et al., 2011; Timmers et al., 2020). Despite these advantages, AAV injection can cause mild or moderate inflammation in the eye. The level of inflammation correlates with the level of dosing: the higher the dosing the higher the inflammation. After a high intravitreal dose of AAV2-sVEGFR-2-Fc (4.7×10^{12} vg/ml) increased immune responses via infiltrating macrophages was seen in the eyes, which is in line with other experiments with viral vectors (Kalesnykas et al., 2017). Clinical inflammatory adverse events of anti-VEGF injections (Cox et al., 2021; Fine et al., 2015) can be treated with topical or systemic corticosteroids (Cox et al., 2021). Moreover, given that sVEGFR-2 is already found naturally (Albuquerque et al., 2009) in ocular and other tissues (albeit not likely at the levels following the transgene expression) the prospect of immune responses against sVEGFR-2-Fc are less likely in human.

In conclusion, we have explored the treatment of ocular neovascularization using sVEGFR-2-Fc expressed by intravitreal AAV2 gene delivery. Gene therapy is an exciting approach to express novel inhibitors of VEGFs, resulting in a greater efficacy and a more sustained effect than intravitreal proteins. However, a greater understanding of the underlying drivers of inflammation and its prevention is needed. The demonstration of AAV2-mediated expression of sVEGFR-2-Fc in the retina and efficacy against CNV is an important step in the development of antiangiogenic gene therapy for patients with ocular neovascular diseases.

Declarations of interest

None.

Data availability

Data will be made available on request.

Acknowledgements

We thank Eila Korhonen for AAV production and Anne Martikainen for technical assistance. This study was supported by Finnish Academy Flagship program (GeneCellNano) and by the Finnish Doctoral Programme in Drug Research.

Appendix A. Supplementary data

Supplementary data to this article can be found online at https://doi.org/10.1016/j.exer.2022.109237.

References

Achen, M.G., Jeltsch, M., Kukk, E., Mäkinen, T., Vitali, A., Wilks, A.F., Alitalo, K., Stacker, S.A., 1998. Vascular endothelial growth factor D (VEGF-D) is a ligand for the tyrosine kinases VEGF receptor 2 (Flk1) and VEGF receptor 3 (Flt4). Proc. Natl. Acad. Sci. U. S. A 95, 548–553. https://doi.org/10.1073/pnas.95.2.548.

Age-related, N., Wykoff, C.C., Clark, W.L., Nielsen, J.S., Booker, J.A., Hunter, M.C., 2018. Journal of Managed C Are & Specialty P Harmacy Optimizing Anti-VEGF Treatment Outcomes for Patients with. KANKSIs Klin, Ophthalmol.

Agostini, H.T., Boden, K., Unsöld, A., Martin, G., Hansen, L.L., Fiedler, U., Esser, N., Marmé, D., 2005. A single local injection of recombinant VEGF receptor 2 but not of Tie2 inhibits retinal neovascularization in the mouse. Curr. Eye Res. 30, 249–257. https://doi.org/10.1080/02713680590923249.

Albuquerque, R.J.C., Hayashi, T., Cho, W.G., Kleinman, M.E., Dridi, S., Takeda, A., Baffi, J.Z., Yamada, K., Kaneko, H., Green, M.G., Chappell, J., Wilting, J., Weich, H. A., Yamagami, S., Amano, S., Mizuki, N., Alexander, J.S., Peterson, M.L., Brekken, R. A., Hirashima, M., Capoor, S., Usui, T., Ambati, B.K., Ambati, J., 2009. Alternatively spliced vascular endothelial growth factor receptor-2 is an essential endogenous inhibitor of lymphatic vessel growth. Nat. Med. 15, 1023–1030. https://doi.org/10.1038/nm.2018.

Askou, A.L., Benckendorff, J.N.E., Holmgaard, A., Storm, T., Aagaard, L., Bek, T., Mikkelsen, J.G., Corydon, T.J., 2017. Suppression of choroidal neovascularization in mice by subretinal delivery of multigenic lentiviral vectors encoding anti-angiogenic MicroRNAs. Hum. Gene Ther. Methods 28, 222–233. https://doi.org/10.1089/hgtb.2017.079.

Askou, A.L., Alsing, S., Benckendorff, J., Holmgaard, A., Mikkelsen, J.G., Aagaard, L., Bek, T., Corydon, T.J., 2019. Suppression of choroidal neovascularization by AAV-based dual-acting antiangiogenic gene therapy. Mol. Ther. Nucleic Acids 16, 38–50. https://doi.org/10.1016/j.omtn.2019.01.012.

Carrasco, J., Pietsch, G.A., Nicolas, M.P., Koerber, C., Bennison, C., Yoon, J., 2020. Real-world effectiveness and real-world cost-effectiveness of intravitreal aflibercept and intravitreal ranibizumab in neovascular age-related macular degeneration: systematic review and meta-analysis of real-world studies. Adv. Ther. 37, 300–315. https://doi.org/10.1007/s12325-019-01147-6.

ClinicalTrials.gov (NCT03066258). Safety and tolerability of RGX-314 gene therapy for neovascular AMD. https://clinicaltrials.gov/ct2/show/NCT03066258?cond=gene+therapy+eye&draw=3&rank=12. (Accessed 3 May 2022).

ClinicalTrials.gov (NCT03585556). AAVCAGsCD59 for the treatment of wet AMD. https://clinicaltrials.gov/ct2/show/study/NCT03585556?cond=gene+therapy+eye&draw=6&rank=47. (Accessed 3 May 2022).

ClinicalTrials.gov (NCT03748784). ADVM-022 intravitreal gene therapy for wet AMD (OPTIC). https://clinicaltrials.gov/ct2/show/NCT03748784. (Accessed 3 May 2022).

ClinicalTrials.gov (NCT04645212). Long-term Study of ADVM-022 in Neovascular (Wet) AMD [OPTIC-EXT]. https://clinicaltrials.gov/ct2/show/NCT04645212. (Accessed 3 May 2022).

Collet, G., Lamerant-Fayel, N., Tertil, M., El Hafny-Rahbi, B., Stepniewski, J., Guichard, A., Foucault-Collet, A., Klimkiewicz, K., Petoud, S., Matejuk, A., Grillon, C., Jozkowicz, A., Dulak, J., Kieda, C., 2013. Hypoxia-regulated overexpression of soluble VEGFR2 controls angiogenesis and inhibits tumor growth. Mol. Cancer Therapeut. 13, 165–178. https://doi.org/10.1158/1535-7163.MCT-13-0637.

Cox, J.T., Eliott, D., Sobrin, L., 2021. Inflammatory complications of intravitreal anti-vegf injections. J. Clin. Med. 10, 1–16. https://doi.org/10.3390/jcm10050981.

Czajkowsky, D.M., Hu, J., Shao, Z., Pleass, R.J., 2012. Fc-fusion proteins: new developments and future perspectives. EMBO Mol. Med. 4, 1015–1028. https://doi.org/10.1002/emmm.201201379.

Ding, K., Shen, J., Hafiz, Z., Hackett, S.F., e Silva, R.L., Khan, M., Lorenc, V.E., Chen, D., Chadha, R., Zhang, M., van Everen, S., Buss, N., Fiscella, M., Danos, O., Campochiaro, P.A., 2019. AAV8-vectored suprachoroidal gene transfer produces widespread ocular transgene expression. J. Clin. Invest. 129, 4901–4911. https://doi.org/10.1172/JCI129085.

Dugel, P.U., Koh, A., Ogura, Y., Jaffe, G.J., Schmidt-Erfurth, U., Brown, D.M., Gomes, A. V., Warburton, J., Weichselberger, A., Holz, F.G., 2020. HAWK and HARRIER: phase 3, multicenter, randomized, double-masked trials of brolucizumab for neovascular age-related macular degeneration. Ophthalmology 127, 72–84. https://doi.org/10.1016/j.ophtha.2019.04.017.

Fine, H.F., Roth, D.B., Shah, S.P., Haque, T., Wheatley, H.M., 2015. Frequency and characteristics of intraocular inflammation after aflibercept injection. Retina 35, 681–686. https://doi.org/10.1097/IAE.0000000000000398.

Heier, J.S., Bressler, N.M., Avery, R.L., Bakri, S.J., Boyer, D.S., Brown, D.M., Dugel, P.U., Freund, K.B., Glassman, A.R., Kim, J.E., Martin, D.F., Pollack, J.S., Regillo, C.D., Rosenfeld, P.J., Schachat, A.P., Wells, J.A., 2016. Comparison of aflibercept, bevacizumab, and ranibizumab for treatment of diabetic macular edema: extrapolation of data to clinical practice. JAMA Ophthalmol 134, 95–99. https://doi.org/10.1001/jamaophthalmol.2015.4110.

Huang, X., Zhou, G., Wu, W., Duan, Y., Ma, G., Song, J., Xiao, R., Vandenberghe, L., Zhang, F., D'Amore, P., Lei, H., 2017. Genome editing abrogates angiogenesis in vivo. Nat. Commun. 8, 112. https://doi.org/10.1038/s41467-017-00140-3.

Kalesnykas, G., Kokki, E., Alasaarela, L., Lesch, H.P., Tuulos, T., Kinnunen, K., Uusitalo, H., Airenne, K., Yla-Herttuala, S., 2017. Comparative study of adeno-associated virus, adenovirus, bacu lovirus and lentivirus vectors for gene therapy of the eyes. Curr. Gene Ther. 17, 235–247. https://doi.org/10.2174/1566523217666171003170348.

Kinnunen, K., Puustjärvi, T., Teräsvirta, M., Nurmenniemi, P., Heikura, T., Laidinen, S., Paavonen, T., Uusitalo, H., Ylä-Herttuala, S., 2009. Differences in retinal neovascular tissue and vitreous humour in patients with type 1 and type 2 diabetes. Br. J. Ophthalmol. 93, 1109–1115. https://doi.org/10.1136/bjo.2008.148841.

Kou, B., Li, Y., Zhang, L., Zhu, G., Wang, X., Li, Y., Xia, J., Shi, Y., 2004. In vivo inhibition of tumor angiogenesis by a soluble VEGFR-2 fragment. Exp. Mol. Pathol. 76 (2), 129–137. https://doi.org/10.1016/j.yexmp.2003.10.010.

Lee, S.H.S., Kim, H.J., Shin, O.K., Choi, J.S., Kim, J., Cho, Y.H., Ha, J., Park, T.K., Lee, J. Y., Park, K., Lee, H., 2018. Intravitreal injection of AAV expressing soluble VEGF receptor-1 variant induces anti-VEGF activity and suppresses choroidal neovascularization. Investig. Ophthalmol. Vis. Sci. 59, 5398–5407. https://doi.org/10.1167/iovs.18-24926.

Lu, F., Adelman, R.A., 2009. Are intravitreal bevacizumab and ranibizumab effective in a rat model of choroidal neovascularization? Graefes Arch. Clin. Exp. Ophthalmol. 247 (2), 171–177. https://doi.org/10.1007/s00417-008-0936-y.

MacLachlan, T.K., Lukason, M., Collins, M., Munger, R., Isenberger, E., Rogers, C., Malatos, S., Dufresne, E., Morris, J., Calcedo, R., Veres, G., Scaria, A., Andrews, L., Wadsworth, S., 2011. Preclinical safety evaluation of AAV2-sFLT01 a gene therapy for age-related macular degeneration. Mol. Ther. 19, 326–334. https://doi.org/10.1038/mt.2010.258.

Millauer, B., Longhi, M.P., Plate, K.H., Shawver, L.K., Risau, W., Ullrich, A., Strawn, L.M., 1996. Dominant-negative inhibition of Flk-1 suppresses the growth of many tumor types in vivo. Cancer Res. 56, 1615–1620.

Mujagic, E., Gianni-Barrera, R., Trani, M., Patel, A., Gürke, L., Heberer, M., Wolff, T., Banfi, A., 2013. Induction of aberrant vascular growth, but not of normal angiogenesis, by cell-based expression of different doses of human and mouse VEGF is species-dependent. Hum. Gene Ther. Methods 24, 28–37. https://doi.org/10.1089/hgtb.2012.197.

Noma, H., Funatsu, H., Mimura, T., Eguchi, S., Shimada, K., 2011. Role of soluble vascular endothelial growth factor receptor-2 in macular oedema with central retinal vein occlusion. Br. J. Ophthalmol. 95 (6), 788–792. https://doi.org/10.1136/bjo.2010.192468.

Papadopoulos, N., Martin, J., Ruan, Q., Rafique, A., Rosconi, M.P., Shi, E., Pyles, E.A., Yancopoulos, G.D., Stahl, N., Wiegand, S.J., 2012. Binding and neutralization of vascular endothelial growth factor (VEGF) and related ligands by VEGF Trap, ranibizumab and bevacizumab. Angiogenesis 15, 171–185. https://doi.org/10.1007/s10456-011-9249-6.

Paterna, J.C., Moccetti, T., Mura, A., Feldon, J., Büeler, H., 2000. Influence of promoter and WHV post-transcriptional regulatory element on AAV-mediated transgene expression in the rat brain. Gene Ther. 7, 1304–1311. https://doi.org/10.1038/sj.gt.3301221.

Rakoczy, E.P., Magno, A.L., Lai, C.M., Pierce, C.M., Degli-Esposti, M.A., Blumenkranz, M. S., Constable, I.J., 2019. Three-year follow-up of phase 1 and 2a rAAV.sFLT-1 subretinal gene therapy trials for exudative age-related macular degeneration. Am. J. Ophthalmol. 204, 113–123. https://doi.org/10.1016/j.ajo.2019.03.006.

Sallinen, H., Anttila, M., Gröhn, O., Koponen, J., Hämäläinen, K., Kholova, I., Kosma, V. M., Heinonen, S., Alitalo, K., Ylä-Herttuala, S., 2011. Cotargeting of VEGFR-1 and -3 and angiopoietin receptor Tie2 reduces the growth of solid human ovarian cancer in mice. Cancer Gene Ther. 18, 100–109. https://doi.org/10.1038/cgt.2010.56.

Schmitt, M., Hippeläinen, E., Raviña, M., Arango-Gonzalez, B., Antopolsky, M., Vellonen, K.S., Airaksinen, A.J., Urtti, A., 2019. Intravitreal pharmacokinetics in mice: SPECT/CT imaging and scaling to rabbits and humans. Mol. Pharm. 16, 4399–4404. https://doi.org/10.1021/acs.molpharmaceut.9b00679.

Shibuya, M., 2011. Vascular Endothelial Growth Factor (VEGF) and its receptor (VEGFR) signaling in angiogenesis: A crucial target for anti- and pro-angiogenic therapies. Genes Cancer 2 (12), 1097–1105. https://doi.org/10.1177/1947601911423031.

Stewart, M.W., 2011. What are the half-lives of ranibizumab and aflibercept (VEGF Trap-eye) in human eyes? Calculations with a mathematical model. Eye Reports 1, 5–7. https://doi.org/10.4081/eye.2011.e5.

Suoranta, T., Laham-Karam, N., Ylä-Herttuala, S., 2021. Optimized protocol for accurate titration of adeno-associated virus vectors. Hum. Gene Ther. 32, 1270–1279. https://doi.org/10.1089/hum.2020.318.

Timmers, A.M., Newmark, J.A., Turunen, H.T., Farivar, T., Liu, J., Song, C., Ye, G.J., Pennock, S., Gaskin, C., Knop, D.R., Shearman, M.S., 2020. Ocular inflammatory response to intravitreal injection of adeno-associated virus vector: relative contribution of genome and capsid. Hum. Gene Ther. 31, 80–89. https://doi.org/10.1089/hum.2019.144.

Toivanen, P.I., Nieminen, T., Viitanen, L., Alitalo, A., Roschier, M., Jauhiainen, S., Markkanen, J.E., Laitinen, O.H., Airenne, T.T., Salminen, T.A., Johnson, M.S., Airenne, K.J., Ylä-Herttuala, S., 2009. Novel vascular endothelial growth factor D variants with increased biological activity. J. Biol. Chem. 284, 16037–16048. https://doi.org/10.1074/jbc.M109.001123.

Wu, Y., Li, Z.Y., Zhao, X., Kan, B., Wei, Y.Q., 2006. Inhibition of ovarian tumor growth by gene therapy with recombinant soluble vascular endothelial growth factor receptor 2. Hum. Gene Ther. 17, 941–948. https://doi.org/10.1089/hum.2006.17.941.

Yu, L., Wu, X., Cheng, Z., Lee, C.V., LeCouter, J., Campa, C., Fuh, G., Lowman, H., Ferrara, N., 2008. Interaction between bevacizumab and murine VEGF-A: a reassessment. Investig. Ophthalmol. Vis. Sci. 49, 522–527. https://doi.org/10.1167/iovs.07-1175.

Zolotukhin, S., Byrne, B.J., Mason, E., Zolotukhin, I., Potter, M., Chesnut, K., Summerford, C., Samulski, R.J., Muzyczka, N., 1999. Recombinant adeno-associated virus purification using novel methods improves infectious titer and yield. Gene Ther. 6, 973–985. https://doi.org/10.1038/sj.gt.3300938.